Supporting Information

Organic electrochemical transistors based on conjugated diketopyrrolopyrrole-dialkoxybithiazole copolymer

Zilan Chen [1], Xiaowei Zhao [1], Chengdong Wang [1], Wenxin Fang [1], Gang Ye[2]*, Lichuan Chen[3], Junyu Li[4], Yanxi Zhang [1]*

Zilan Chen, Xiaowei Zhao, Chengdong Wang, Wenxin Fang, Yanxi Zhang

[1]Institute of Flexible Electronics (IFE, Future Technologies), Xiamen University, Xiamen 361005, China.

E-mail: ifeyxzhang@xmu.edu.cn

Gang Ye

[2]Key Laboratory for the Green Preparation and Application of Functional Materials, Hubei Key Laboratory of Polymer Materials, School of Materials Science and Engineering, Hubei University, Youyi Road 368, Wuhan, 430062 China

E-mail: g.ye0612@hubu.edu.cn

[3]Lichuan Chen

State Key Laboratory of Physical Chemistry of Solid Surfaces, College of Chemistry and Chemical Engineering, Xiamen University, Xiamen 361005, China.

[4]Junyu Li

Sinopec Shanghai Research Institute of Petrochemical Technology, Shanghai 201028, China.

1. Synthesis and Characterization of materials

Reagents

All reagents and solvents were commercial and were used as received. 4,4'-bis(octyloxy)-2,2'-bis(trimethylstannyl)-5,5'-bithiazole (Tz) were purchased from SunaTech. 3,6-bis(5-bromothiophen-2-yl)-2,5-bis(2-(2-(2-ethoxyethoxy)ethoxy)ethyl)pyrrolo[3,4-c]pyrrole-1,4(2H,5H)-dione (DPPTEG-Br) was synthesized according to the literature.[1,2]

Characterization

^{1}HNMR and ^{13}CNMR were performed on a Bruker AV-500 spectrometer at 25 °C, using tetramethylsilane (TMS) as an internal standard. NMR shifts are reported in ppm, relative to the residual protonated solvent signals of $CDCl_3$ (δ= 7.26 ppm) or at the carbon absorption in $CDCl_3$ (δ = 77.23 ppm). Multiplicities are denoted as: singlet (s), doublet (d), triplet (t) and multiplet (m). GPC measurements were conducted on a Waters ACQUITY APC room temperature GPC/SEC system in the United States at 30 °C, using hexafluoroisopropanol (HFIP) as the eluent compared to polystyrene standards.

Cyclic voltammetry (CV) was carried out with a CHI760 Evoltammetric potentiostat in a three-electrode configuration where the working electrode was platinum disk electrode, the counter electrode was a platinum wire, and the pseudo-reference was an Ag wire that was calibrated against ferrocene/ferrocenium redox (Fc/Fc^{+}). Cyclic voltammograms for the D-A copolymer films deposited on the glassy carbon working electrode in $CHCN_3$ solution containing Bu_4NPF_6 (0.1 mol L^{-1}) electrolyte at a scanning rate of 50 mV s^{-1}.

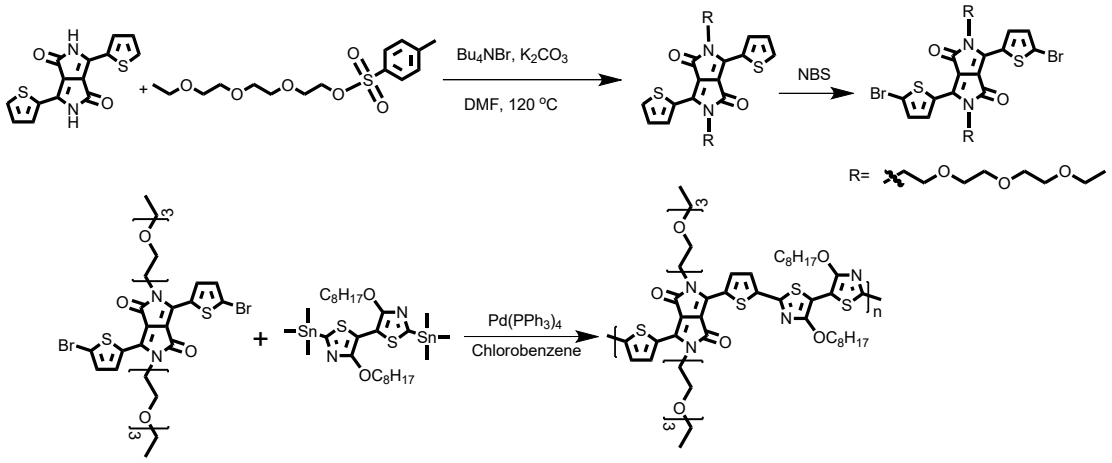

Scheme S1. Synthetic route for DPP-based monomer and polymers.

General Synthetic Procedures for the DPP based Polymers

To a dry three-neck flask, DPP based monomer (0.1 mmol) and thiophene based monomer (0.1 mmol) were added under argon followed by tris(dibenzylideneacetone) dipalladium [$Pd_2(dba)_3$] (6.4 mg) and tri(o-tolyl)phosphine [$P(o\text{-tolyl})_3$] (9.6 mg). The flask and its contents were subjected to 3 pump/purge cycles with N_2 followed by addition of anhydrous, degassed chlorobenzene (5 mL) via syringe. The reaction mixture was stirred at 120 °C for three days. After cooling to room temperature, the deeply green colored reaction mixture was dropped into 100 mL vigorously stirred methanol (containing 5 mL 12 M hydrochloride acid). After stirring for 4 hours, the precipitated solid was collected by filtration. The solid polymers were re-dissolved in chloroform and reprecipitated into methanol. After filtration, the polymers were subjected to sequential Soxhlet extraction. The sequential solvents were methanol, hexane and chloroform. Impurities and low-molecular-weight fractions were removed by methanol and hexane. Finally, the polymer solution in chloroform was concentrated to give the polymers as dark solid.

PDPP-TEG-Tz Synthesis according to the general polymerization procedure: monomer DPPTEG-Br (78 mg, 0.1 mmol), monomer Tz (75 mg, 0.1 mmol), dry chlorobenzene (5 mL). The polymer was obtained as a dark solid (96 mg, 92 %).

^{1}HNMR (400 MHz, $CDCl_3$): δ 10.85-8.00 (m, 4H), 5.03-2.63 (m, 32H), 3.32-0.32 (m, 32H).

GPC: Mn = 256 kDa, Mw = 322 kDa, PDI = 1.26.

FT-IR (cm^{-1}) 680, 709, 730, 798, 862, 1014, 1057, 1235, 1258, 1347, 1399, 1435, 1465, 1488, 1544, 1663, 2853, 2921.

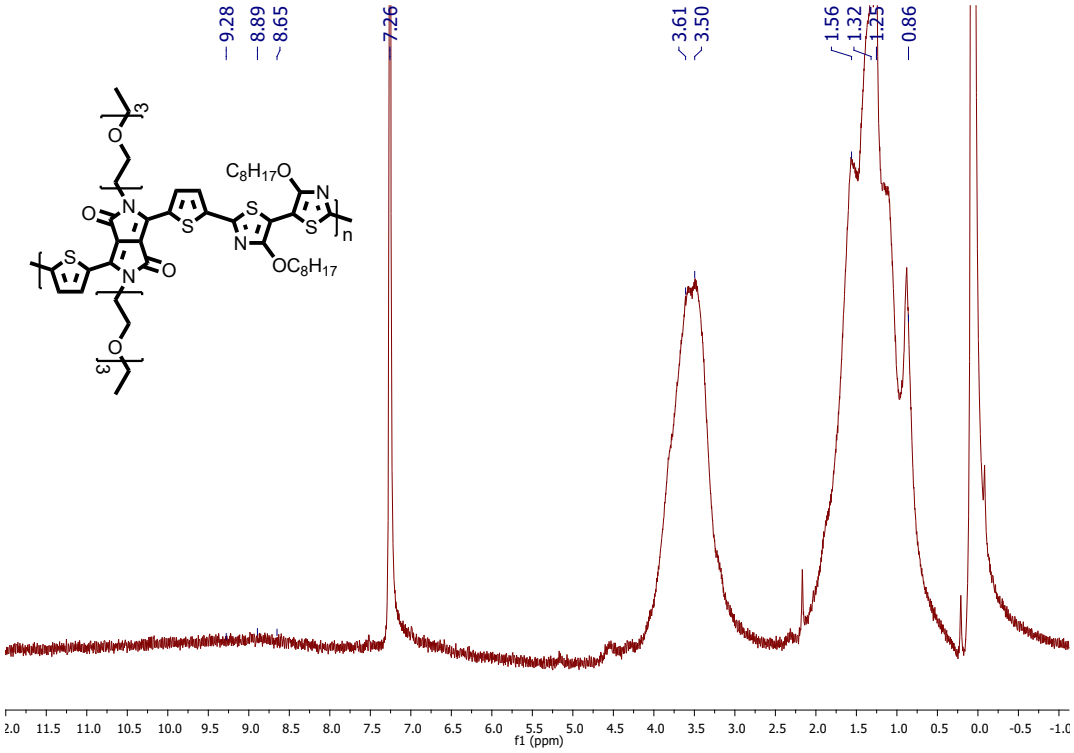

Figure S1. ^{1}HNMR spectra of PDPP-TEG-2Tz.

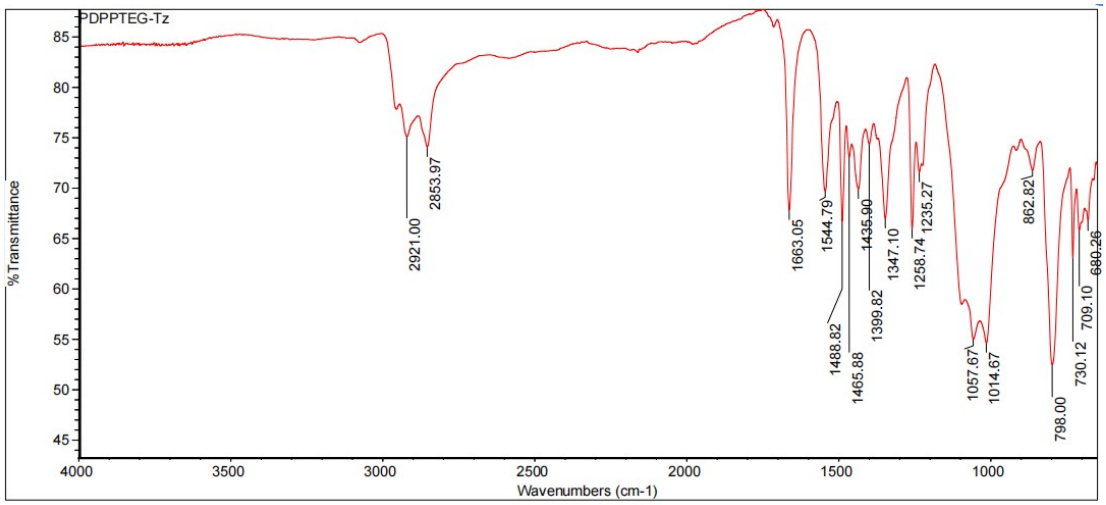

Figure S2. IR spectra of PDPP-TEG-2Tz.

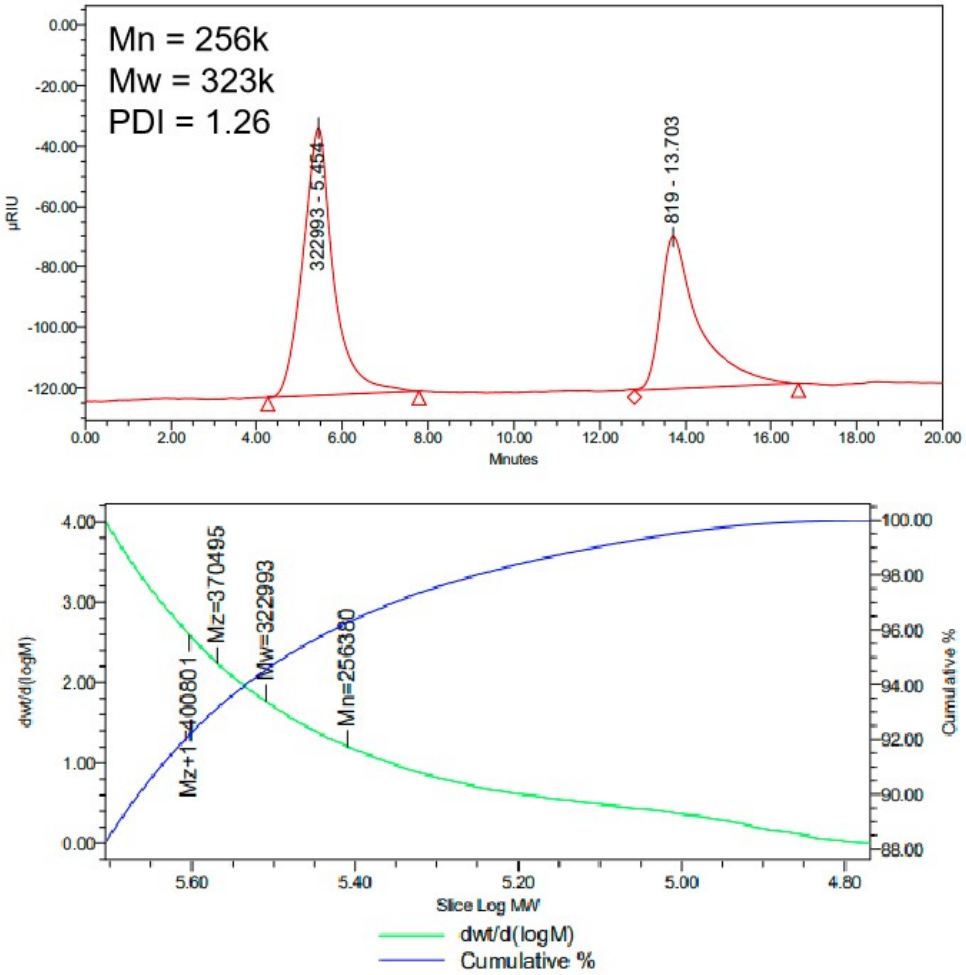

Figure S3. GPC trace of PDPP-TEG-2Tz.

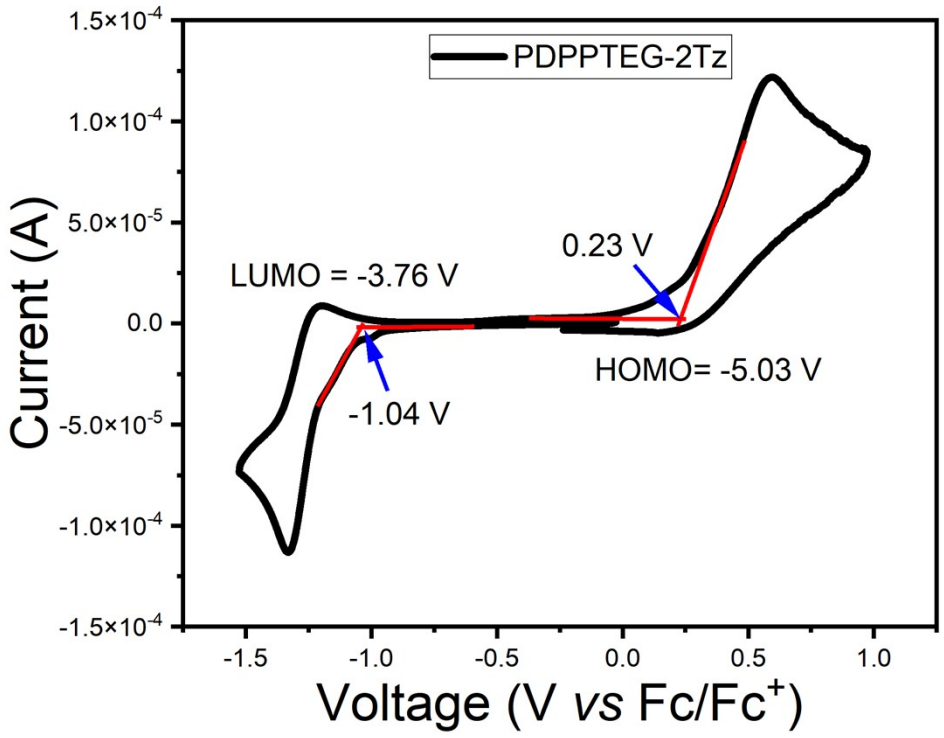

Figure S4. Cyclic voltammetry of polymer thin films (PDPP-TEG-2Tz) on glass carbon substrates in $CHCN_3$ solution containing Bu_4NPF_6 electrolyte.

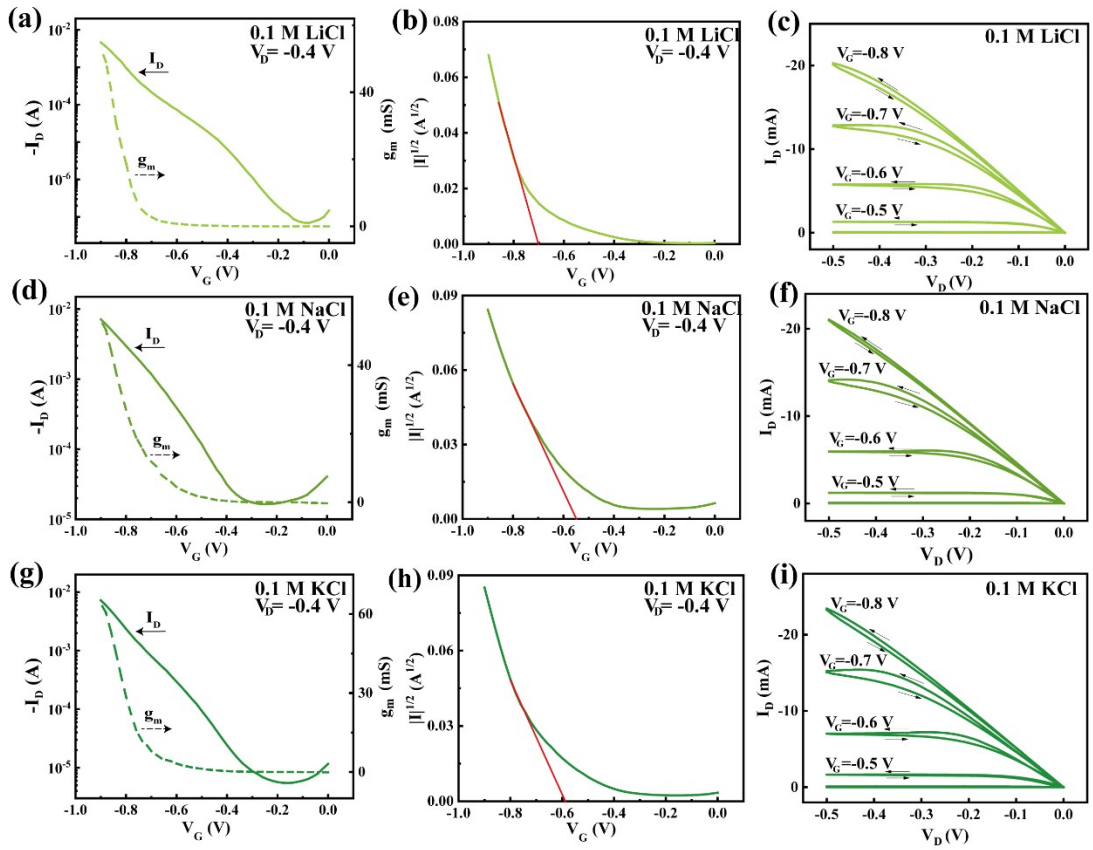

Figure S5. (a-i) OECT characteristics of three electrolytes, each containing different cations (Li^+, Na^+, K^+) , while sharing the same anion (Cl^-) at an identical concentration (0.1 M). This investigation encompassed the analysis of transport curves, correlation transconductance, and output curves.

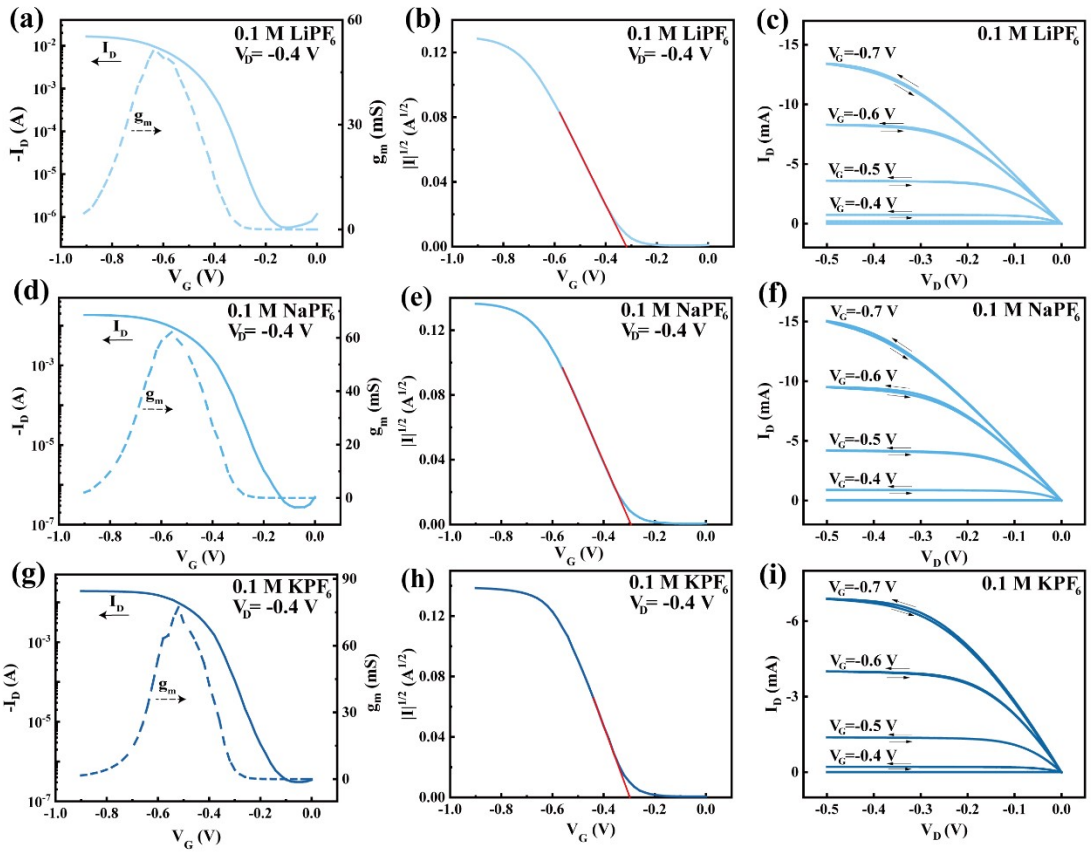

Figure S6. (a-i) OECT characteristics of three electrolytes , each containing different cations (Li^+, Na^+, K^+) , while sharing the same anion (PF_6^-) at an identical concentration (0.1 M). This investigation involved the analysis of transport curves, correlation transconductance, and output curves.

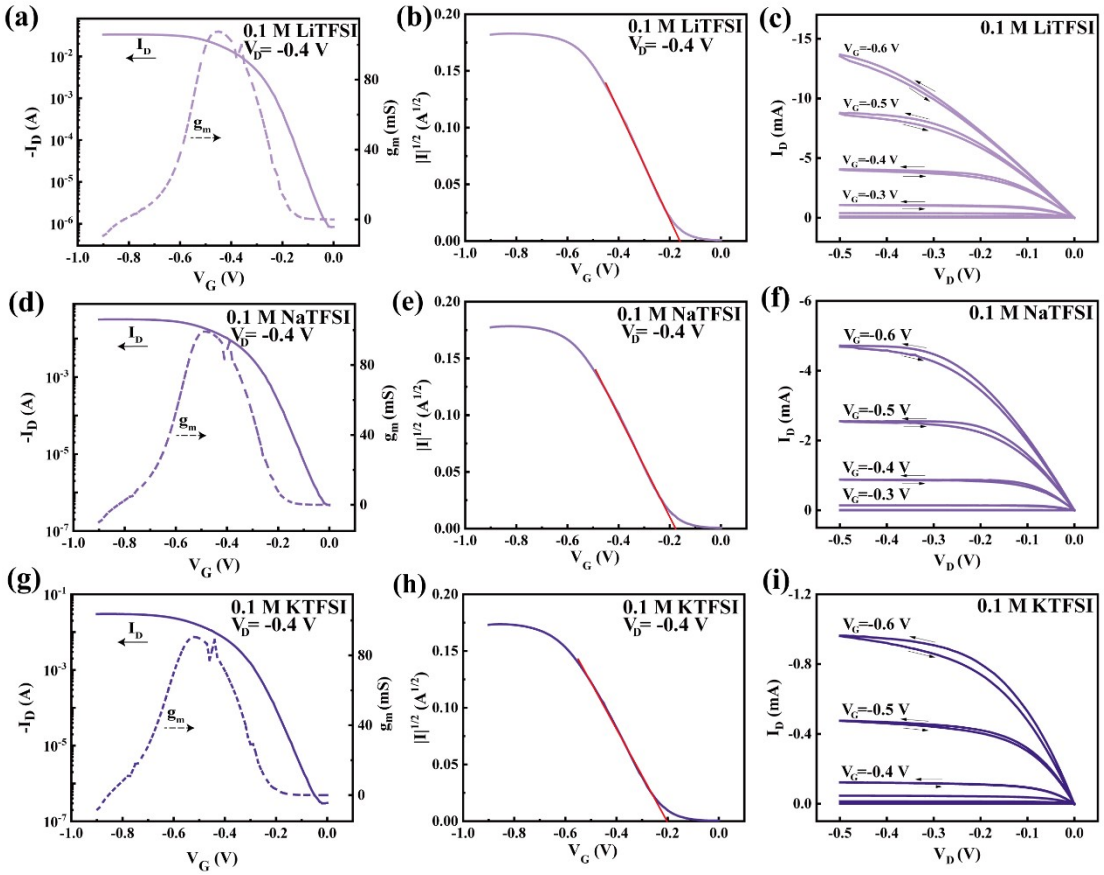

Figure S7. (a-i) OECT characteristics of three electrolytes , each containing different cations (Li^+, Na^+, K^+) , while sharing the same anion ($TFSI^-$) at an identical concentration (0.1 M). This investigation involved the analysis of transport curves, correlation transconductance, and output curves.

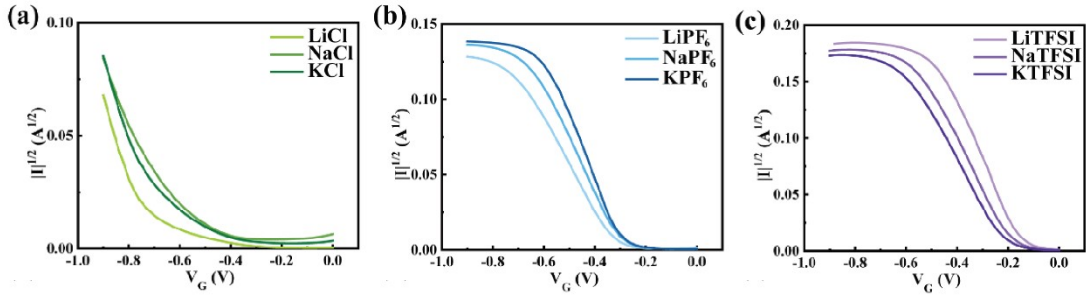

Figure S8. Threshold voltages were extracted from the transfer curves obtained using various ion types of electrolytes. (a-c) Comparison results for the same anion (Cl^-, PF_6^-, $TFSI^-$) with different cations (Li^+, Na^+, K^+).

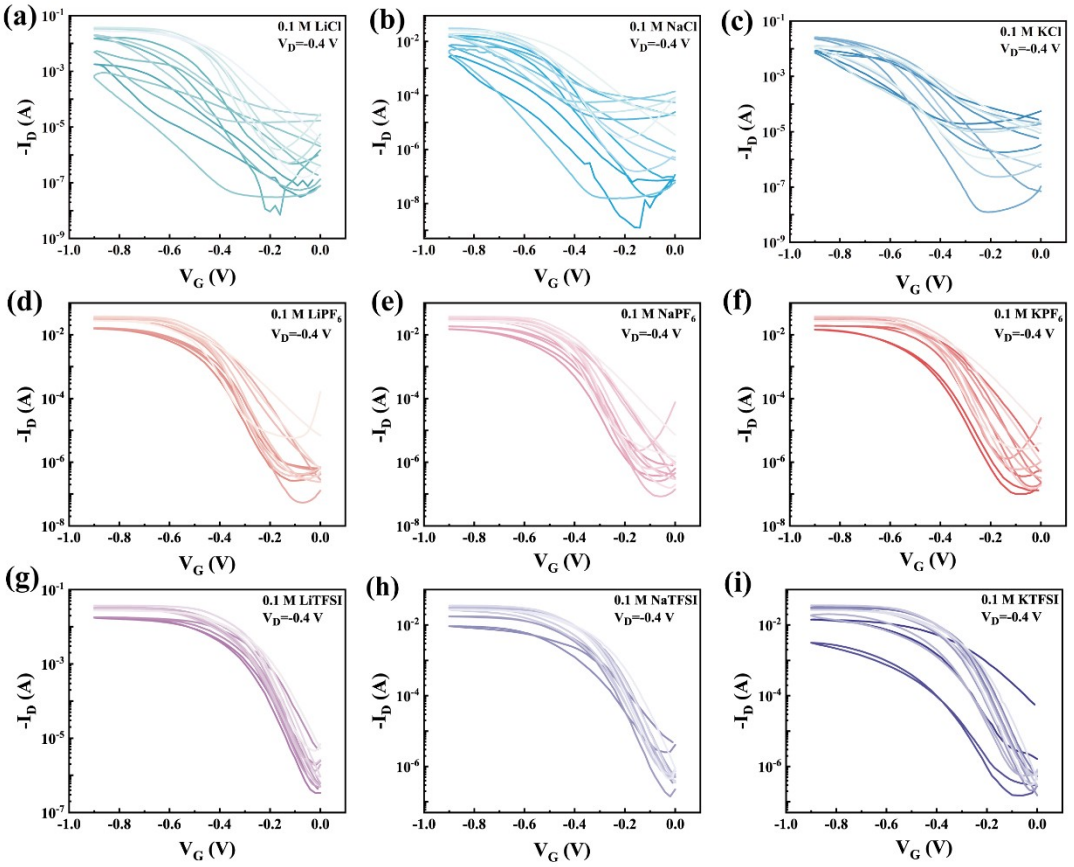

Figure S9. Transfer characteristics of OECTs of nine different electrolytes at the same concentration (0.1 M) were plotted on a logarithmic scale to represent ON/OFF ratio of drain currents. In addition, at least seven different OECT devices were measured in each electrolyte, and each results of each measurement were distinguished by different colored lines.

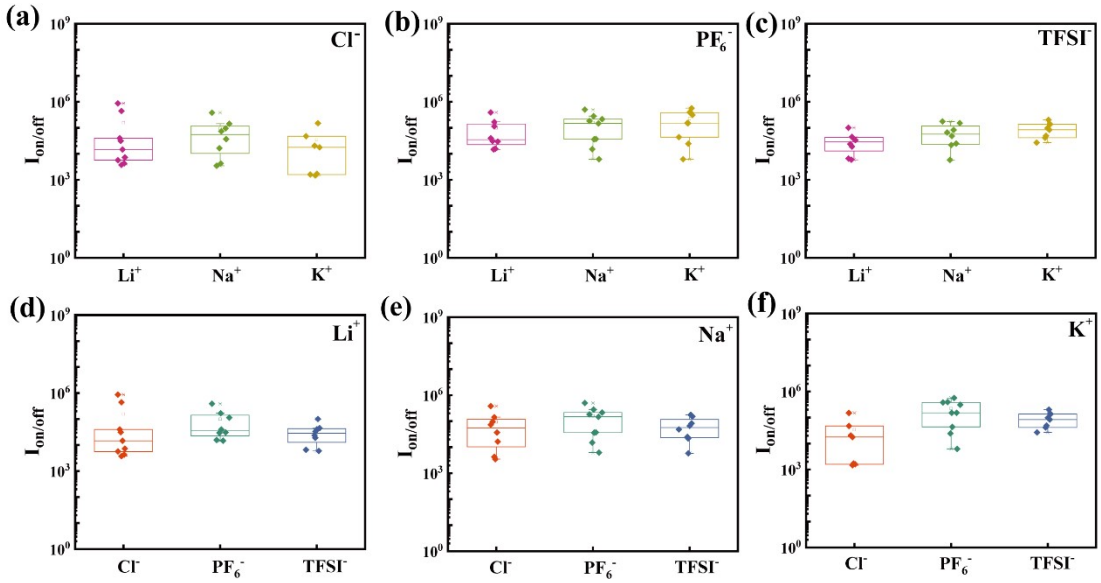

Figure S10. Box plot shows the switching ratios of p-OECT devices for different electrolyte measurements. Each dot represents a separate OECT. (a-c) Comparison results of the same anion (Cl^-, PF_6^-, $TFSI^-$) with different cations (Li^+, Na^+, K^+). (d-f) Comparison of the same cation (Li^+, Na^+, K^+) with different anions (Cl^-, PF_6^-, $TFSI^-$). For box plots, center line is median; box limits are 25th and 75th percentiles; whiskers are outliers within 25th and 75th percentile + 1.5x interquartile range; "□" is the average; "x" represents maximum and minimum values.

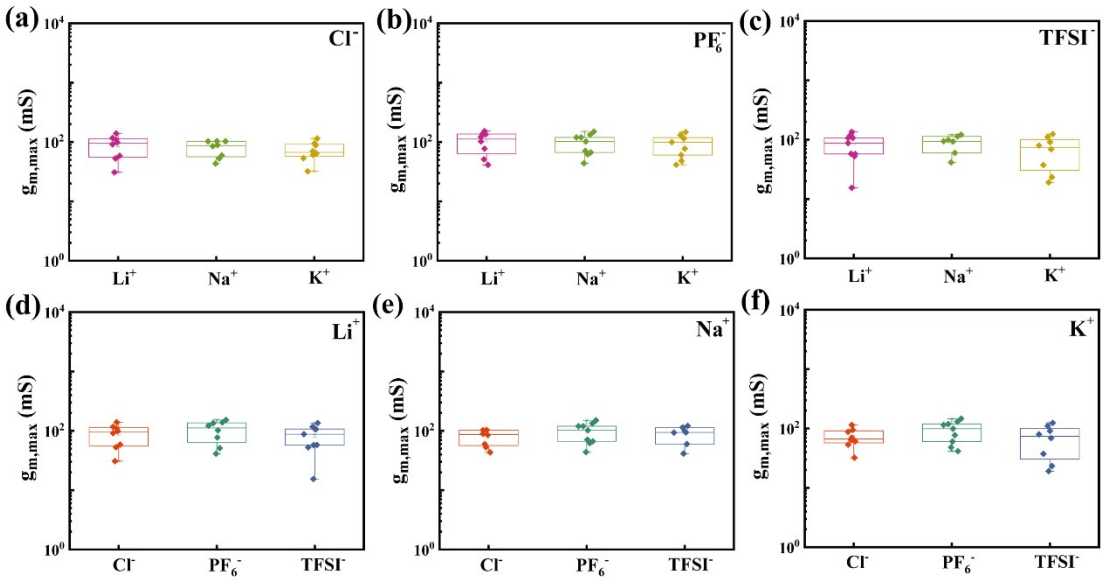

Figure S11. Box plot shows the results of the maximum transconductance of p-OECT devices measured with different electrolytes. Each dot represents a separate OECT. (a-c) Comparison results of the same anion (Cl^-, PF_6^-, $TFSI^-$) and different cations (Li^+, Na^+, K^+). (d-f) Comparison of the same cation (Li^+, Na^+, K^+) and different anions (Cl^-, PF_6^-, $TFSI^-$). For box plots, center line is median; box limits are 25th and 75th percentiles; whiskers are outliers within 25th and 75th percentile + 1.5x interquartile range; "□" is the average; "x" represents maximum and minimum values.

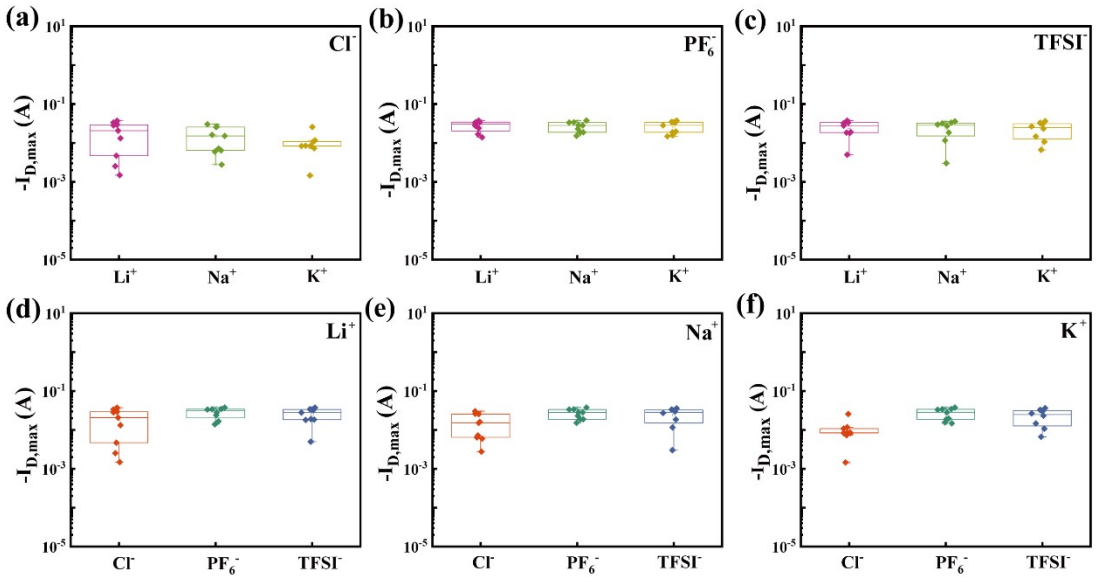

Figure S12. Box plot shows the maximum current acquired at the source-drain electrode for p-OECT devices measured with different electrolytes. Each dot represents a separate OECT. (a-c) Comparison results of the same anion (Cl^-, PF_6^-, $TFSI^-$) and different cations (Li^+, Na^+, K^+). (d-f) Comparison of the same cation (Li^+, Na^+, K^+) and different anions (Cl^-, PF_6^-, $TFSI^-$). For box plots, center line is median; box limits are 25th and 75th percentiles; whiskers are outliers within 25th and 75th percentile + 1.5x interquartile range; "□" is the average; "x" represents maximum and minimum values.

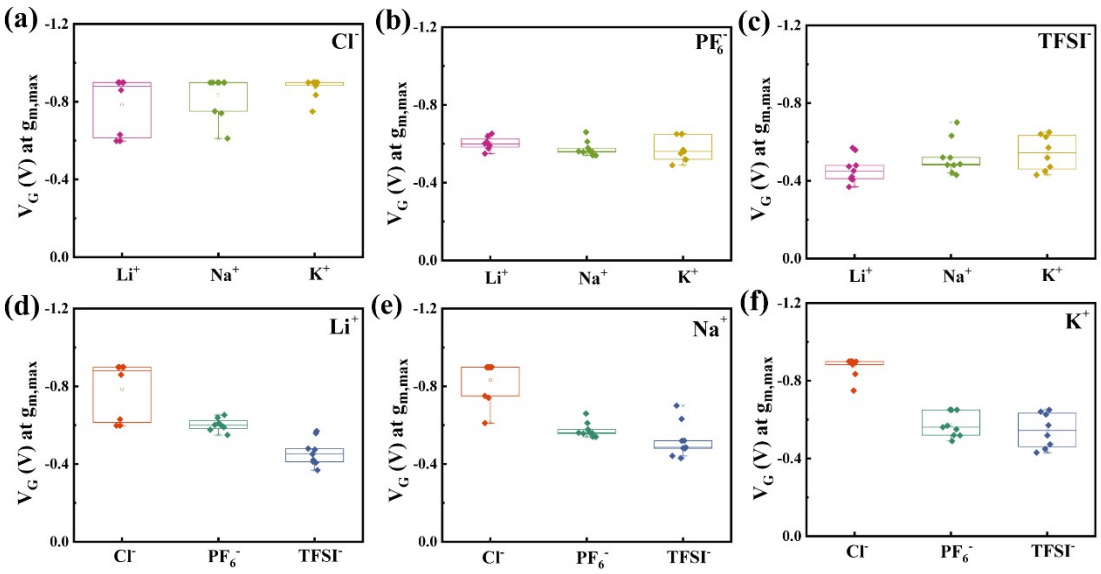

Figure S13. Box plot shows the results for the threshold voltage at the maximum transconductance of p-OECT devices measured with different electrolytes. Each dot represents a separate OECT. (a-c)

Comparison results of the same anion (Cl^-, PF_6^-, $TFSI^-$) and different cations (Li^+, Na^+, K^+). (d-f) Comparison of the same cation (Li^+, Na^+, K^+) and different anions (Cl^-, PF_6^-, $TFSI^-$). For box plots, center line is median; box limits are 25th and 75th percentiles; whiskers are outliers within 25th and 75th percentile + 1.5x interquartile range; "□" is the average; "x" represents maximum and minimum values.

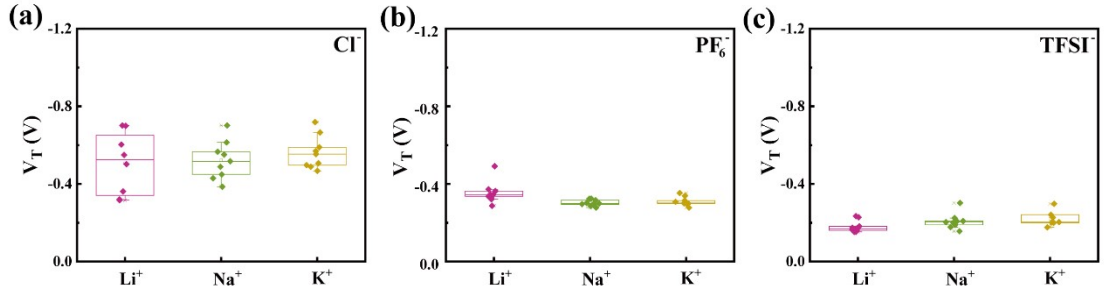

Figure S14. Box plot shows the results of the threshold voltages for p-OECT devices measured in different electrolytes. Each dot represents a separate OECT. (a-c) Comparison results of the same anion (Cl^-, PF_6^-, $TFSI^-$) and different cations (Li^+, Na^+, K^+). For box plots, center line is median; box limits are 25th and 75th percentiles; whiskers are outliers within 25th and 75th percentile + 1.5x interquartile range; "□" is the average; "x" represents maximum and minimum values.

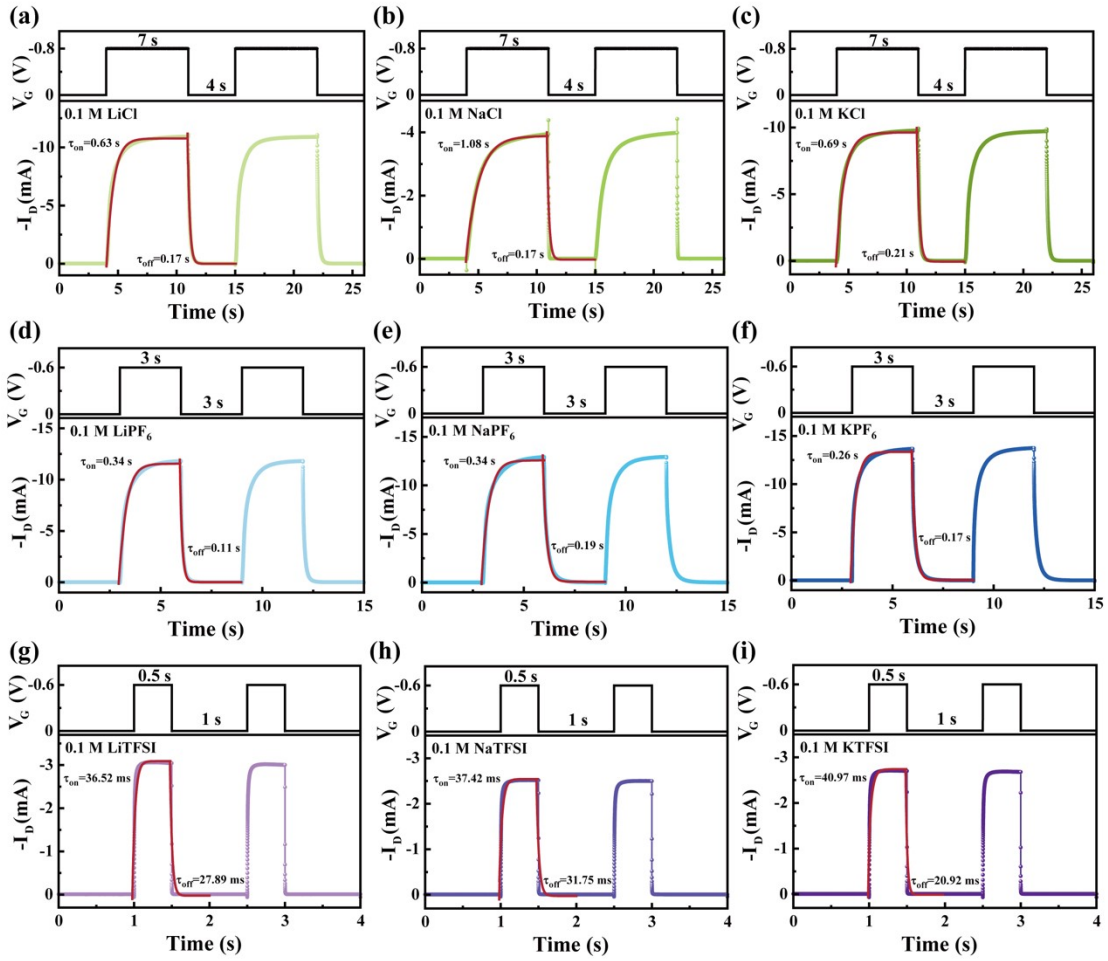

Figure S15. Transient response characteristics of PDPP-TEG-2Tz-based OECTs in nine different 0.1 M electrolytes, analyzed by measuring the drain current under specific pulse conditions. For chloride anion (Cl^-), V_G=-0.8 V was used, while for hexafluorophosphate (PF_6^-) and bis(trifluoromethanesulfonyl)imide ($TFSI^-$), V_G=-0.6 V was applied, corresponding to their respective threshold voltages (see Figure 3d-f). Notably, V_D = -0.4 V corresponds to the saturation region in the output curves of OECTs.

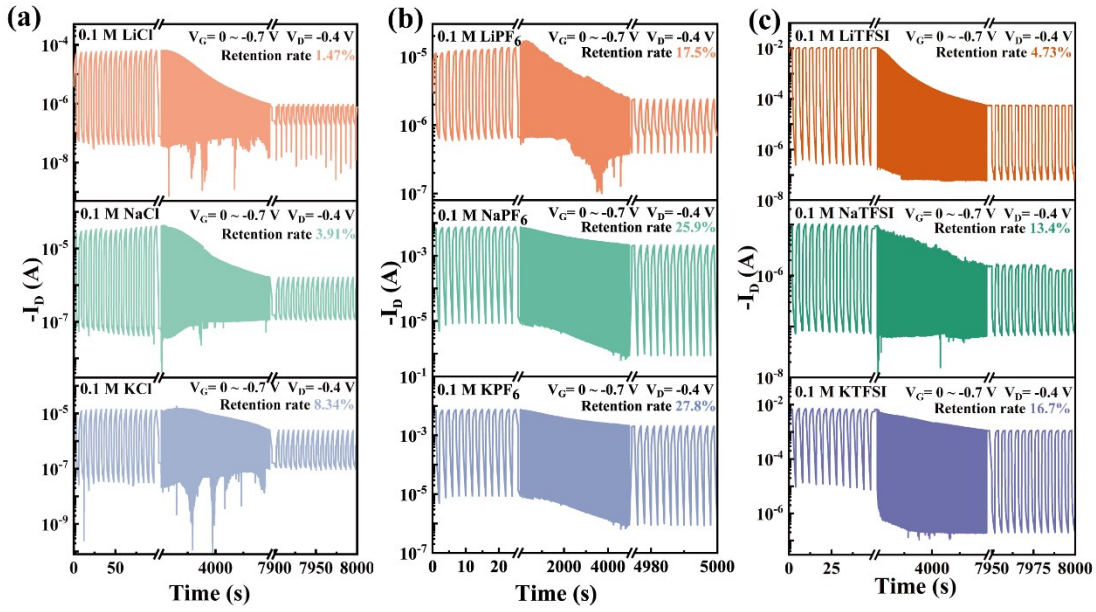

Figure S16. Stability of p-OECT devices were assessed by conducting continuous measurements over more than 5000 pulses in nine different electrolytes at a concentration of 0.1 M. During these measurements, V_G varied from 0 to -0.7 V, V_D was set to -0.4 V, and the pulse widths were adjusted as follows: 3 s for Cl^-, 1s for PF_6^-, $TFSI^-$. The pulse length was maintained at 50 ms, and the device operated normally throughout the measurement period.

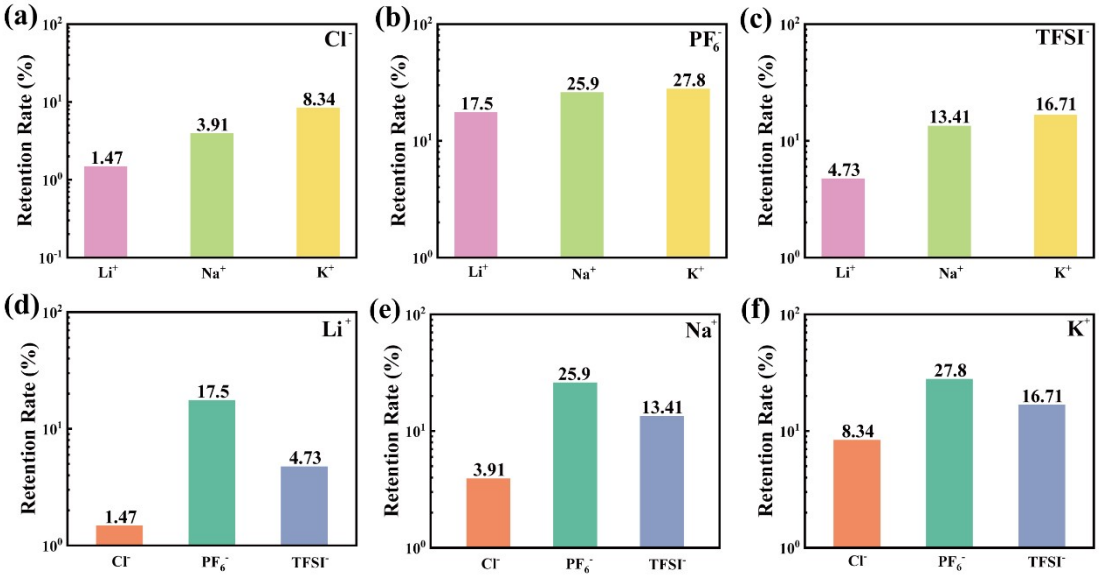

Figure S17. Columns charts show the extraction of current retention parameters from the stability measurements of different electrolytes, as shown in Figure S16. (a-c) Comparison results of the same

anion (Cl^-, PF_6^-, $TFSI^-$) and different cations (Li^+, Na^+, K^+). (d-f) Comparison of the same cation (Li^+, Na^+, K^+) and different anions (Cl^-, PF_6^-, $TFSI^-$).

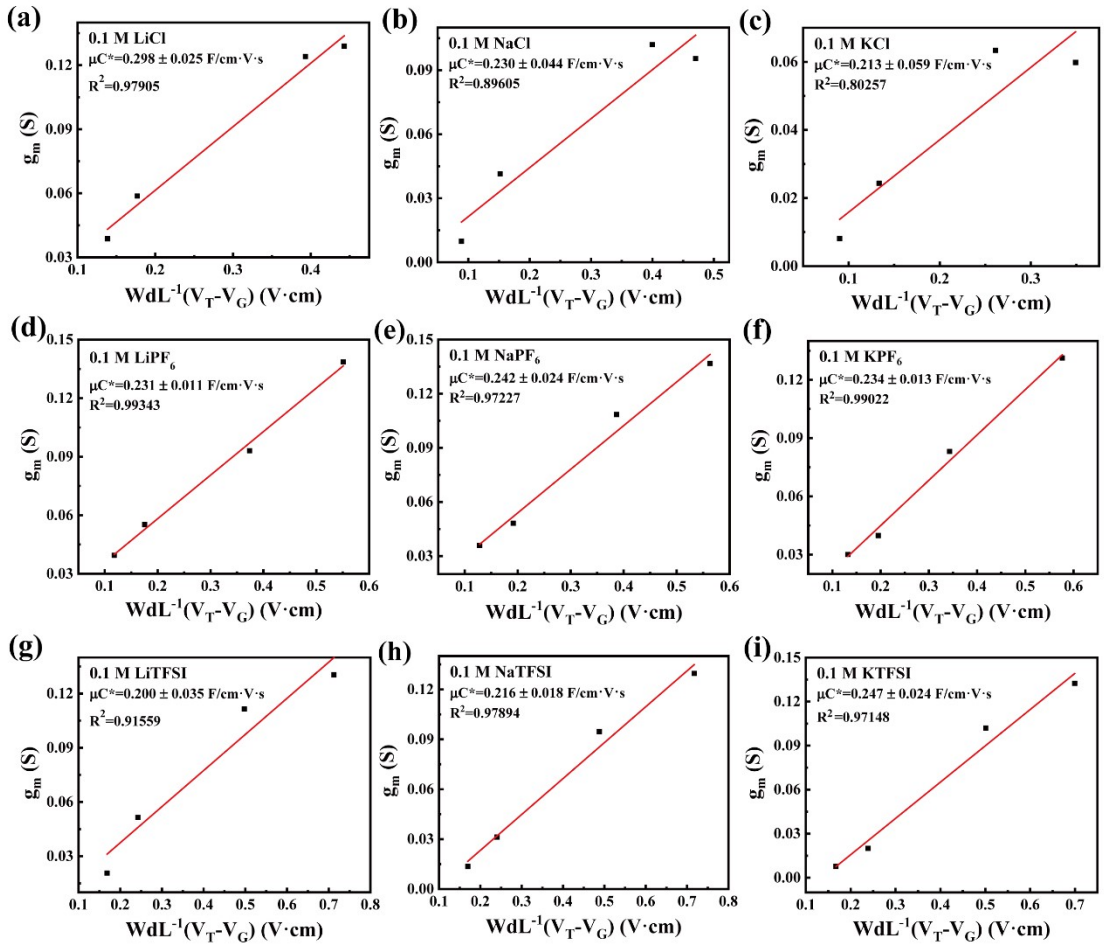

Figure S18. (a-i) μC* values of OECTs based on the PDPP-TEG-2Tz polymer in different types of electrolyte solutions, all at the same concentration (0.1 M). Each data point on the graph represents a transistor device.

Table S1. Summary of OECT properties of PDPP-TEG-2Tz based on different electrolytes.

Elektrolyte (0.1 M)	$I_{on/off}$	V_T (V)	$g_{m,norm}$ (S cm^{-1})	g_m (mS)	μC* (F $cm^{-1}V^{-1}s^{-1}$)	τ_{on} (s)	τ_{off} (s)
LiCl	~10^3	-0.51±0.16	1.46±0.61	87.16±36.67	0.298±0.025	0.63	0.17
NaCl	~10^3	-0.52±0.10	1.33±0.40	79.85±24.41	0.230±0.044	1.08	0.17
KCl	~10^3	-0.56±0.08	1.20±0.43	72.13±25.90	0.213±0.059	0.69	0.21
$LiPF_6$	~10^4	-0.36±0.06	1.71±0.70	102.27±41.79	0.231±0.011	0.34	0.11
$NaPF_6$	~10^4	-0.30±0.02	1.61±0.61	96.37±36.78	0.242±0.024	0.34	0.19

KPF_6	~10^4	-0.31±0.02	1.55±0.63	92.91±37.72	0.234±0.013	0.26	0.17
LiTFSI	~10^4	-0.18±0.03	1.37±0.64	81.90±38.44	0.200±0.035	0.037	0.028
NaTFSI	~10^4	-0.21±0.04	1.48±0.48	88.88±28.63	0.216±0.018	0.037	0.032
KTFSI	~10^4	-0.22±0.04	1.16±0.66	69.23±39.51	0.247±0.024	0.041	0.021

Table S2. The molecular packing parameters for PDPP-TEG-2Tz, detailing the out-of-plane (OOP).

Solid-state packing (100)	PDPP-TEG-2Tz (OPP)
q (nm^{-1})	3.84
d-spacing (nm)	1.58
FWHM (nm^{-1})	0.999
Correlation length (nm)	2.0
g	0.11

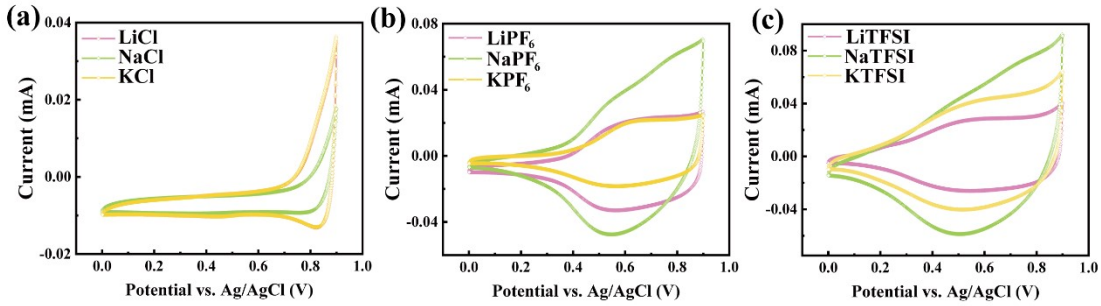

Figure S19. Cyclic voltammetry measurements (CVs) were conducted in aqueous electrolytes containing various anions at identical concentrations (0.1 M). Ten CV cycles were executed with a scan rate of 100 mV/s, ranging from 0 V to 0.9 V.(a-c) Comparison of the same anions (Cl^-, PF_6^-, $TFSI^-$) and different cations (Li^+, Na^+, K^+).

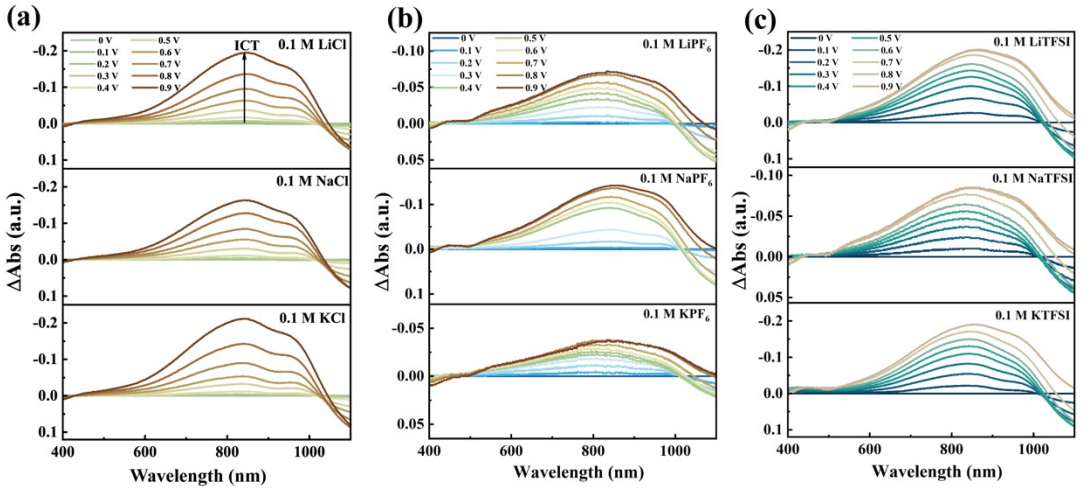

Figure S20. Electrochemical doping level was determined by spectroelectrochemistry. In a 0.1 M aqueous solution containing nine different electrolytes, the relative absorbance of PDPP-TEG-2T films at various wavelengths was compared for different anions (Cl^-, PF_6^-, $TFSI^-$). The PDPP-TEG-2T film was deposited on an ITO/glass substrate as the working electrode, with Ag/AgCl as the reference and counter electrodes. Taking the 0.1 M LiCl electrolyte as an example, the relative absorbance of as-cast PDPP-TEG-2Tz film across various wavelengths, with an applied voltage ranging from 0 V to 0.9 V in 0.1 V increments. The vertical arrows highlight the evolution of the spectral characteristics of the polymer's ICT transition at 850 nm. The evolution of the relative intensity of absorption peaks at 850 nm (ICT-top) as the gate bias increases.

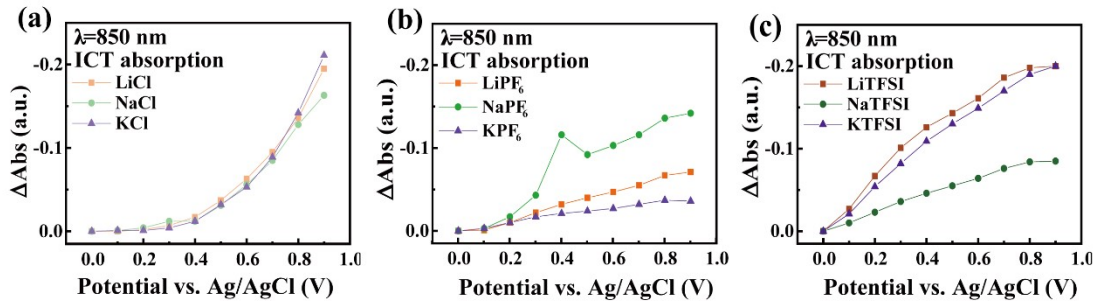

Figure S21. Electrochemical doping level was assessed using spectroelectrochemistry. (a-c) Comparison of the same anions (Cl^-, PF_6^-, $TFSI^-$) and different cations (Li^+, Na^+, K^+). The evolution of relative

intensity of absorption as the gate bias increases in the intramolecular charge transfer and polarons absorption (bottom) extracted from spectroelectrochemistry at 850 nm when the polymer is in contact with different electrolytes.

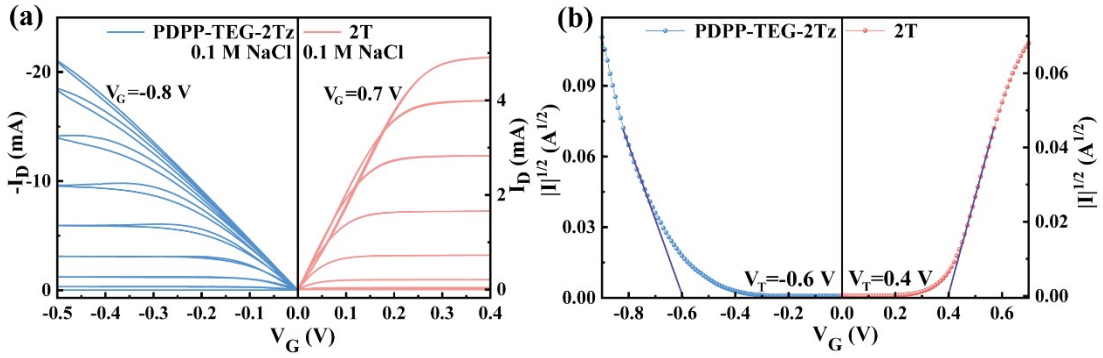

Figure S22. Performance matching of OECT-based complementary channel materials. (a) Output curves of PDPP-TEG-2Tz (p-type) and PNDI2C8TEG-2T (2T, n-type). (b) Intercept is extracted on the x-axis as the threshold voltage of OECT devices according to the respective $\sqrt{I_D}$ as a function of gate voltage (V_G).

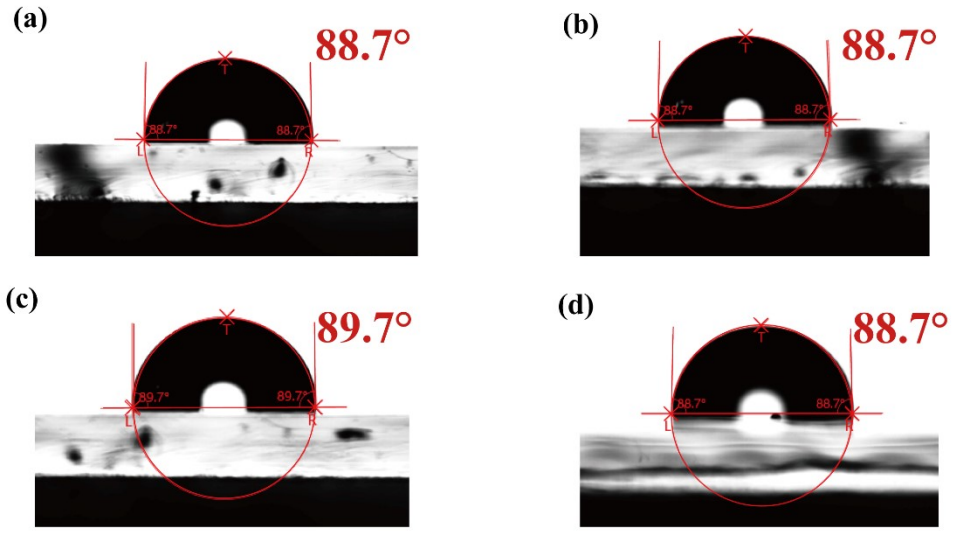

Figure S23. Water Contact Angle Tests. (a-d) Results from tests on the same sample at four different locations. The results indicate that even with TEG hydrophilic side chains functionalizing the polymer, the material retains hydrophobic properties, indicative of weak water-material interaction. This suggests

the TEG chains lack sufficient density or uniform surface distribution, failing to significantly alter the material's hydrophobicity. Such characteristics may impair device performance. Future work will focus on increasing TEG chain density, optimizing their polymer distribution, and conducting targeted surface treatments to enhance the development and application of D-A structure conjugated polymers with thiazole (Tz) donors.

References

(1) Mei, J.; Graham, K. R.; Stalder, R.; Tiwari, S. P.; Cheun, H.; Shim, J.; Yoshio, M.; Nuckolls, C.; Kippelen, B.; Castellano, R. K.; Reynolds, J. R. Self-Assembled Amphiphilic Diketopyrrolopyrrole-Based Oligothiophenes for Field-Effect Transistors and Solar Cells. *Chem. Mater.* **2011**, *23* (9), 2285–2288.

(2) Kanimozhi, C.; Yaacobi-Gross, N.; Chou, K. W.; Amassian, A.; Anthopoulos, T. D.; Patil, S. Diketopyrrolopyrrole–Diketopyrrolopyrrole-Based Conjugated Copolymer for High-Mobility Organic Field-Effect Transistors. *J. Am. Chem. Soc.* **2012**, *134* (40), 16532–16535.